Molecular Glue-Augmented E2-Ubiquitin Recognition from A Computational Approach

Danial Muhammad[1,2,3†], Wei Xia[4,5†], Musheng Wang[1,2,3], Zhaoxi Sun[1,2]*, and John Z.H. Zhang[1,2,3,4,5*]

[1]*Faculty of Synthetic Biology, Shenzhen University of Advanced Technology, Shenzhen 518107, China*

[2]*Key Laboratory of Quantitative Synthetic Biology, Shenzhen Institute of Synthetic Biology, Shenzhen Institutes of Advanced Technology, Chinese Academy of Sciences, Shenzhen 518055, China*

[3]*University of Chinese Academy of Sciences, Beijing 100049, China*

[4]*New York University–East China Normal University Center for Computational Chemistry, School of Chemistry and Molecular Engineering, New York University Shanghai, 1555 Shiji Road, Pudong New Area, Shanghai 200124, China*

[5]*Department of Chemistry, New York University, New York, New York 10003, United States.*

†These authors contributed equally to this paper.

*To whom correspondence should be addressed:

John Z. H. Zhang john.zhang@nyu.edu

Zhaoxi Sun z.sun@pku.edu.cn

Abstract

Ubiquitin (Ub) is a small regulatory protein that tags unwanted or misfolded proteins for degradation by the proteasome. Molecular glues as small molecules stabilizing and augmenting protein-protein interactions have gained increasing attention in ubiquitination. Highly efficient computational approaches for the investigation of thermodynamics of molecular glue (MG)-Ub-protease systems remain absent. In this work, we introduced a cost-effective computational framework for all-atom characterization of the thermodynamics driving force in the cooperativity or molecule glue-induced enhancement of Ub-E2 recognition. Based on the testing bed involving the CDC34A-Ub protein-protein system and 18 unique molecule glues, we illustrate that our method could satisfactorily decoding the interaction thermodynamics inside the multimeric system. Specifically, our method enables both the ranking the protein-ligand MG-(E2-Ub) affinity and qualitatively capture the MG-induced E2-Ub interaction strengthening, which are generally unachievable with standard methods such as MM/GBSA and commonly applied scoring functions (e.g., AutoDock Vina). We additionally explore the general picture of the

interfacial interactions in the multimeric complex, identifying important residues in the binding of molecular glue to Ub-E2 complex and also in Ub-E2 binding. Our computational approach could facilitate high-throughput virtual screening of potent molecular glues in assisting protein-protein recognition and ubiquitination.

Keywords: Molecular Glue, Ubiquitin, Protein-protein Interaction, Protein-ligand Binding, Cooperativity

1. Introduction.

Cancer remains a leading cause of mortality worldwide, representing a significant global health challenge. According to the World Health Organization (WHO) in 2020, cancer is the second most common cause of death worldwide, accounting for 10 million deaths annually.[1] This underscores the persistent burden of cancer on public health systems worldwide. In the United States alone, an estimated 1,665,540 individuals were diagnosed with cancer in 2013, with 585,720 succumbing to the disease within the same year.[2] Among the various types of cancer, lung cancer exhibits a high prevalence, affecting both men and women.[3] The WHO classifies lung cancer into two primary subtypes based on morphological and biological characteristics: small-cell lung cancer and non-small-cell lung cancer.[4] Despite significant advancements in lung cancer treatment modalities, the 5-year survival rate remains disappointingly low, at less than 15%.[5]

The Ubiquitin-proteasome system is crucial for maintaining cellular protein homeostasis (proteostasis) in eukaryotes, regulating key processes like cell proliferation, DNA repair, and stress response.[6] This proteolytic system tags proteins with ubiquitin (Ub), marking them for degradation by the 26S proteasome.[7] This involves a multi-step enzymatic cascade involving E1 (ubiquitin-activating), E2 (ubiquitin-conjugating), and E3 (ubiquitin ligase) enzymes. E2 enzymes such as CDC34A (UBE2R1) are charged with Ub and subsequently transfer it to cullin-RING ligases (CRL), facilitating substrate ubiquitination.[8, 9] Dysregulation of E2 can accelerate Ub turnover and promote the degradation of p27, a cyclin-dependent kinase (CDK) inhibitor, leading to uncontrolled cancer cell proliferation.[10] Overexpression of E2 has been observed in various cancers, including lung, liver, and breast cancers, implicating its role in tumorigenesis.[11-13] Stable E2-Ub interactions prevent the transfer of E2 to CRLs, disrupting cancer cell growth and survival and consequently highlighting E2 as a promising therapeutic target.[14]

Small molecules typically interact with a limited number of hot-spot residues that contribute significantly to the binding energy.[15, 16] Despite progress in small-molecule targeted anti-cancer drugs, challenges like low response rates and drug resistance remain significant hurdles.[17] The structure determination of CC0651-E2-Ub complex unexpectedly reveals that the small molecule inhibitor (CC0651) stabilizes the low-affinity interaction between the E2 and Ub,[18] which would increase the efficiency of ubiquitination and facilitate the degradation of disease-causing proteins (see Fig. 1A for a schematic illustration of the MG-induced stabilization of the Ub-E2 protein-protein complex). Consequently, such small molecules introducing additional stabilization effects

to protein-protein complexes are named as molecular glues (MG), facilitating the selective degradation of oncogenic proteins and disrupting pathways critical to tumor growth and survival.[19]

Computational modelling has emerged as one of the key components in modern drug discovery.[20-23] Rational drug design relies heavily on accurately quantifying protein-ligand interactions and prediction of binding affinities through in silico methods.[24-28] The situation could be especially difficult for the specific E2-Ub-MG complex due to its multimeric and complicated-constituent nature, i.e., involving both protein-ligand and protein-protein complexes. Despite the applications of modern computational techniques such as umbrella sampling to construct the free energy profiles, it still lacks a protocol with balanced computational burden and accuracy. To fill this critical gap, we attempt to employ an generalized alanine scanning with generalized Born and interaction entropy (ASGB-IE)[29, 30] technique for the multimeric protein-protein-ligand complex. The numerical outcomes suggest that our method is able to not only accurately rank the protein-ligand affinity, but also qualitatively capture the MG-induced stabilization of the protein-protein complex. We additionally provide detailed energetic perspectives about the key residues stabilizing the protein-MG complex and more importantly probing the additional MG-induced residue-specific stabilization effects, providing effectively a comprehensive structure-activity relationship (SAR) analysis. By assessing the contribution of each residue within the binding pocket, this approach aims to uncover key interactions within the ternary complex and provide crucial insights into the Ub loading and unloading mechanisms of E2.

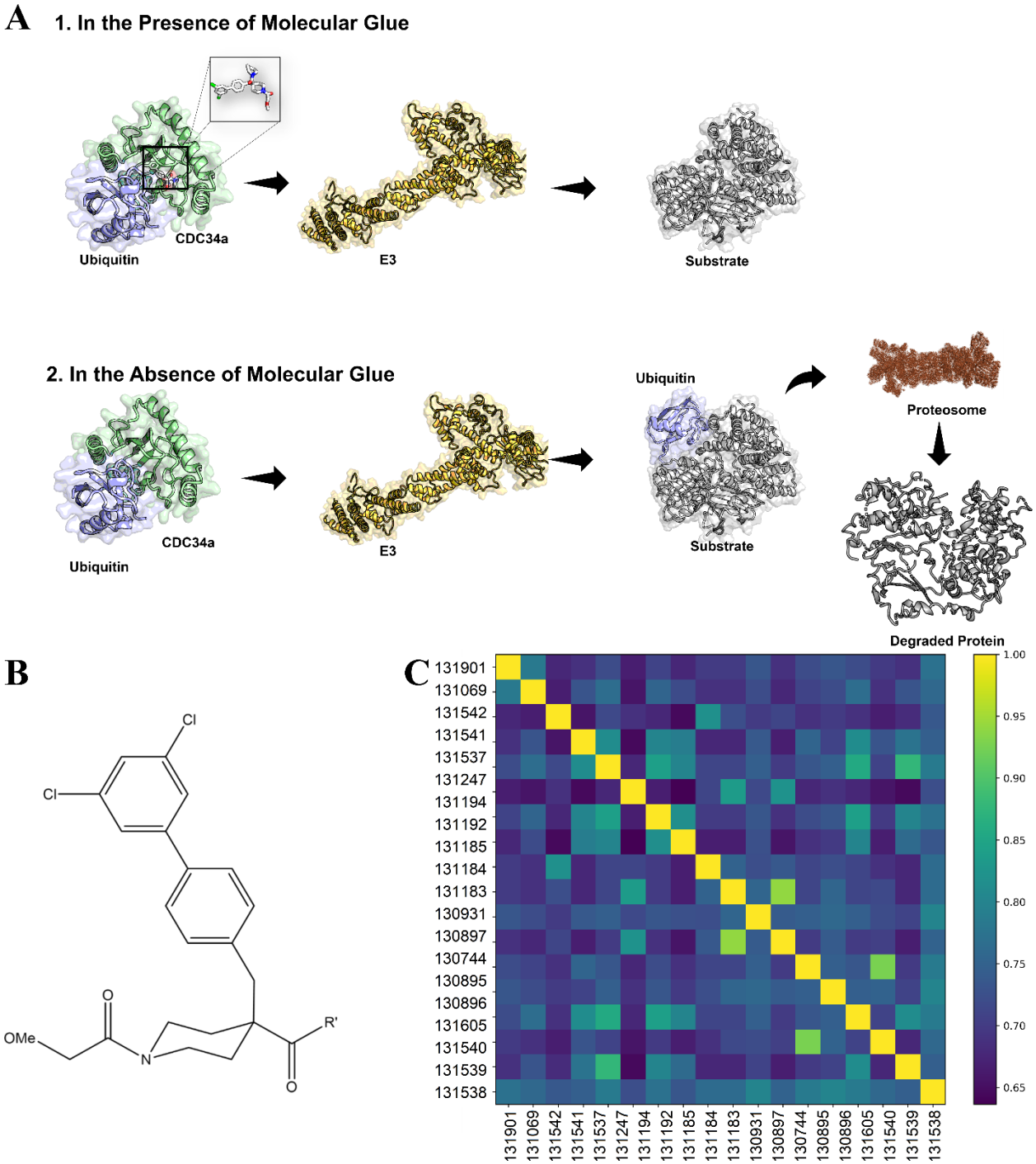

Fig. 1. A) An illustration of the molecular glue-enhanced protein-protein binding. The ubiquitin-protease pathway is inhibited upon the addition of MG. B) 2D structures of template glue investigated in this work. C) The Tanimoto similarity map depicting similarities and diversities of investigated molecular glues.

2. Methodology.

2.1. Binding cooperativity from an ASGB-IE approach.

The protein-protein interaction (PPI) between E2 (CDC34A) and Ub could be stabilized by MG, which would inhibit the Ub-proteasome pathway[31] and thus alter biological functions. This ligand binding-induced PPI strength could be understood as a cooperative effect, the quantification of which requires the estimation of interaction thermodynamics in E2-Ub, E2-MG and Ub-MG pairs in the bound state and the E2-Ub interaction in the unbound state. The central thermodynamic property of interest in the MG-induced cooperative effect is

$$\Delta G_{cooperativity} = \Delta G_{bind}^{E2-Ub+M} - \Delta G_{bind}^{E2-Ub} \quad (1).$$

To understand this process, we introduce a cooperativity-involved ASGB-IE[29, 30, 32] framework. The base computational alanine scanning-based technique involves the mutational scanning (alanine to be specific) of interfacial residues close to the interaction site(s). The thermodynamic variation during the *x* (wild type) to *a* (alanine) mutation could be written as

$$\Delta\Delta G_{bind}^{x\to a} = \Delta G_{bind}^{a} - \Delta G_{bind}^{x} \quad (2).$$

Following an end-point decomposition procedure, the formula could be transformed to

$$\Delta\Delta G_{bind}^{x\to a} = \Delta\Delta G_{gas}^{x\to a} + \Delta\Delta G_{sol}^{x\to a} \quad (3),$$

where the *gas* (gas-phase) and *sol* (solvation) contributions are separated. Individual terms could be further decomposed into

$$\Delta\Delta G_{gas}^{x\to a} = \Delta G_{gas}^{a} - \Delta G_{gas}^{x} \quad (4a).$$

$$\Delta\Delta G_{sol}^{x\to a} = \Delta G_{sol}^{a} - \Delta G_{sol}^{x} \quad (4b).$$

The gas-phase terms could be computed using the interaction entropy method[30, 32]

$$\Delta G_{gas}^{i} = \langle E_{int}^{i} \rangle - T\Delta S_{int}^{i} = \langle E_{int}^{i} \rangle - \frac{1}{\beta}\ln\left\langle e^{\beta\Delta E_{i}^{int}} \right\rangle \quad (5),$$

where the variable *i* could be either *x* or *a*, the subscript int denotes the interaction energies between different components of the system (e.g., proteins and MG) and the brackets represent ensemble average. Under a force-field framework, the interaction energy could be further decomposed into electrostatic and vdW interactions, i.e.,

$$\Delta E_{i}^{int} = \Delta E_{i}^{ele} + \Delta E_{i}^{vdW} \quad (6).$$

The solvation contribution could be computed following the common practice in end-point free energy calculations, i.e., the implicit-solvent generalized Born (GB) technique (the GB^{OBC} parametrization[33, 34], to be specific) for the polar contribution in conjunction with the linear

surface-area formula[35] for the non-polar solvation work. To account for the polarization effects, in end-point practices it is common to alter the dielectric constants for the protein interior, and we follow our previous best practices using 1, 3 and 5 for charged, polar and apolar residues[29].

The contribution of individual residues defined by Eq. (2) provides an estimate of the energetic drop upon the alanine mutation, thus quantifying the importance of the selected residue in interfacial coordination. Based on this energetics, it is common to define the hotness of the spot, i.e., classifying into hot, warm or cold spots. A commonly employed threshold for hot spots is 1 kcal/mol. The overall binding free energy could be calculated by summation of the contributions of individual residues

$$\Delta G_{bind} = -\sum_x \Delta\Delta G_{bind}^{x\to a} \quad (7).$$

Consequently, the MG-induced affinity elevation in the E2-Ub complex could be written as

$$\Delta G_{cooperativity} = -\sum_x^{E2-Ub+M} \Delta\Delta G_{bind}^{x\to a} + \sum_x^{E2-Ub} \Delta\Delta G_{bind}^{x\to a} \quad (8).$$

In brief, while in previous ASGB-IE calculations the scanning target could be either protein-ligand and protein-protein systems, the scanning target in the current multimeric protein-protein-ligand complex is generalized. When investigating the protein stabilization of the ligand (i.e., protein-ligand) binding, the scanning target is the protein-protein complex and the binding affinity of MG to the E2-Ub complex is obtained with

$$\Delta G_{bind}^{M-(E2-Ub)} = -\sum_x^{M-(E2-Ub)} \Delta\Delta G_{bind}^{x\to a} \quad (9).$$

By contrast, when investigating the protein-protein interaction, the scanning targets in the PPI system is residues in both protein chains. In all alanine scanning, we follow the common practice using a distance threshold of 5 Å, i.e., including all interfacial residues within 5 Å from the binding target in the mutational scan.

2.2. Molecular Simulations.

Homology modelling of the E2-Ub-MG complex is conducted based on the X-ray diffraction structure 7M2K, in which the missing residues are modeled using the loop modeler of the MOE software. Hydrogens were added to the structure, and the structure was prepared using the quick prep module of MOE[1, 36, 37]. In the following presentations, we have the first 169 residues as E2 and the 170-244 residues as Ub. For molecular glues, in total we consider 18 molecules sharing the same backbone/template shown in Fig. 1B. The structures and EC50 values of these molecules from experimental reference[31] are summarized in Table S1. The ligand similarity map (the

Tanimoto regime with RDKit) is shown in Fig. 1C, where a certain level of diversity could be observed. The structure modification (e.g., alkyl group addition) is performed with the Schrodinger Maestro.

As discussed in the previous section, we consider both the ternary complex E2-Ub-MG and the ordinary protein-protein complex E2-Ub in our modelling. So, we have two types of simulation cells (the MG-unbound and MG-bound states). Each simulation cell is constructed using AMBER14SB[38] to describe the protein, AM1-BCC[39, 40] charges and GAFF2 to describe ligands (molecular glues), TIP3P water for solvation and monovalent sodium/chloride ions[41, 42] parametrized for the water model for neutralization. For the non-standard amino acids featuring the multiple methyl groups in the lysine side chain, we employed the existing parameters published in references.[43] Then, we conduct minimization to get rid of unfavorable interactions, 250 ps constant-volume heating to 300 K and 50 ns NPT equilibration are performed, after which a triplicate 50 ns sampling with a 50 ps snapshot interval is performed. The final estimates are reported as the averaged results of the three replicas. We employ SHAKE[44, 45] constraints on bonds involving hydrogen, Langevin dynamics for temperature regulation, isotropic scaling and Monte Carlo barostat for pressure regulation at 1 atm, and the 10 Å real-space cutoff for non-bonded interactions. The hybrid-precision GPU version of pmemd in AMBER is used for molecular simulations.

For post-processing energetic evaluation, we employ the above-mentioned ASGB-IE framework and also the standard MM/GBSA protocol, where no entropic contribution is calculated. Additionally, we benchmark several common scoring functions applied in molecular docking, including the well-known AutoDock Vina, its Vinardo alternative[46, 47], the refitted dkoes_scoring version available in smina, and the contact-based PRODIGY-LIG[48] scoring function.

3. Results and discussion.

The detailed ASGB-IE energetics of all systems are summarized in Table S2-S37. As noted above, the first 169 residues are E2 and the 170-244 residues are Ub. A convergence check is performed by comparing the all-frame (i.e., 1000) estimate and that using only a fraction of it (200-frame) of ASGB-IE-computed protein-protein E2-Ub binding (with/without MG) for all

systems in Fig. S1. A near perfect correlation is observed, which indicates the satisfactory convergence behavior of our end-point free energy estimates.

3.1. Binding Strengths in E2-Ub-MG Multimeric Systems.

For any computational method to work, it is of utmost importance to first validate the results with direct comparison to experiment. We therefore first probe the quality of calculation of the MG-(E2-Ub) binding strength following Eq. (9) in Fig. 2, based on three statistical metrics including Pearson r, Spearman r_s and Kendall τ. While ASGB-IE achieves a good correlation (Pearson) and also a good ranking behavior (Kendall and Spearman), the correlation coefficients of MM/GBSA are rather poor. Interestingly, the well-known AutoDock families (Vina, Vinardo and the dkoes_scoring refit) and the empirical contact-based scoring function PRODIGY-LIG achieve performances better than MM/GBSA but still worse than ASGB-IE. This phenomenon highlights the applicability of our computational framework.

With the established solidity (reproducing experimental protein-ligand affinity), we then investigate the MG-induced augmentation of protein-protein (E2-Ub) binding strength. The calculation generally follows Eq. (8), and the numerical data are shown in Fig. 2B. For the ASGB-IE energetics, it is clearly shown that all glue molecules are introducing additional stabilization effects into the E2-Ub packing, with several molecules (e.g., 130931) achieving the largest augmenting effects. However, this MG-induced E2-Ub protein-protein affinity increase is not captured by MM/GBSA. This again validates the superiority of ASGB-IE in modelling the thermodynamics in multimeric MG-involved systems. The absence of experimental data on this cooperative effect presents a direct comparison, but it is safe to conclude that the ASGB-IE calculations effectively capture the additional stabilization effects.

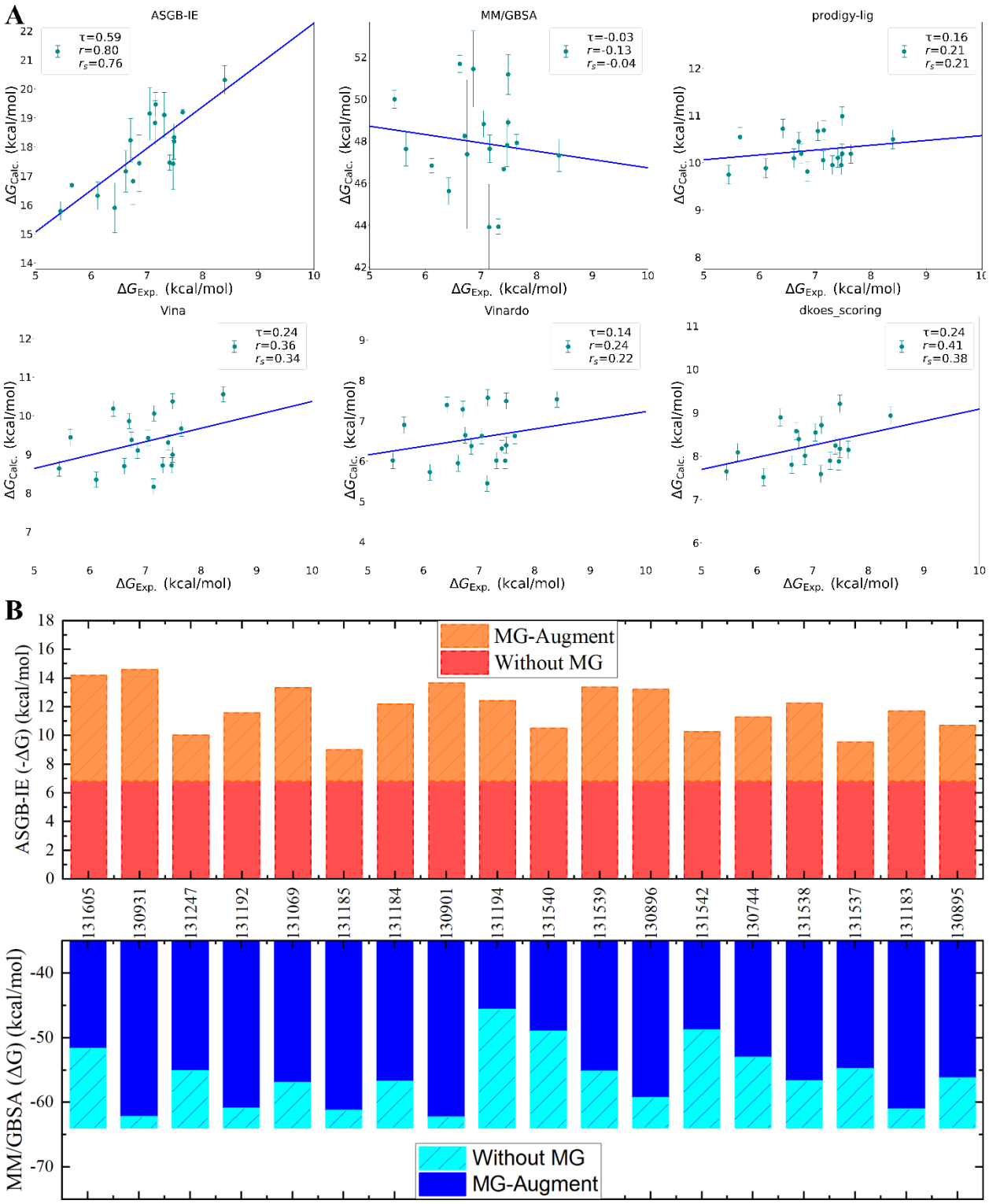

Fig. 2. A) Correlograms of calculated estimates of MG-(E2-Ub) binding strengths and experimental affinities using ASGB-IE, MM/GBSA, three AutoDock scoring functions (Vina, Vinardo and dkoes_scoring) and PRODIGY-LIG. The three quality metrics and the best linear fit

are also presented. B) Protein-protein affinities in the presence and absence of MG and the affinity increase upon the binding of MG calculated with ASGB-IE and MM/GBSA.

3.2. Key Protein-MG interactions stabilizing the multimeric system.

While the above thermodynamic data are generally in good agreement with experimental observation, it is desirable to grasp more detailed insights with atomic details, which is also the strength of all-atom simulations compared with experimental measurements. To this aim, we pick the E2-Ub-131605 complex as an example due to its highest protein-MG binding affinity (see Table S1). Please refer to Fig. 3A for a 3D illustration of the protein-MG complex. Alanine scanning reveals that 42PRO, 46TYR, 47TYR, 117ASN and several other residues make the large contributions to the protein-MG binding (c.f., Fig, 3B). The top-4 residues have a binding free energy generally larger than the empirical rule (1 kcal/mol) and thus could be considered as hot spots. According to the 2D interaction map shown in Fig. 3C, the nature of the protein-MG interactions are mainly hydrophobic contacts and aromatic π-π stacking forces. An interesting phenomenon to note is that most of residues with high energetic contributions are on the E2 protein, and only one residue 218LYS is on Ub. This is not an expected fact, as MG is closer to E2 and interacts with mostly protein residues on E2.

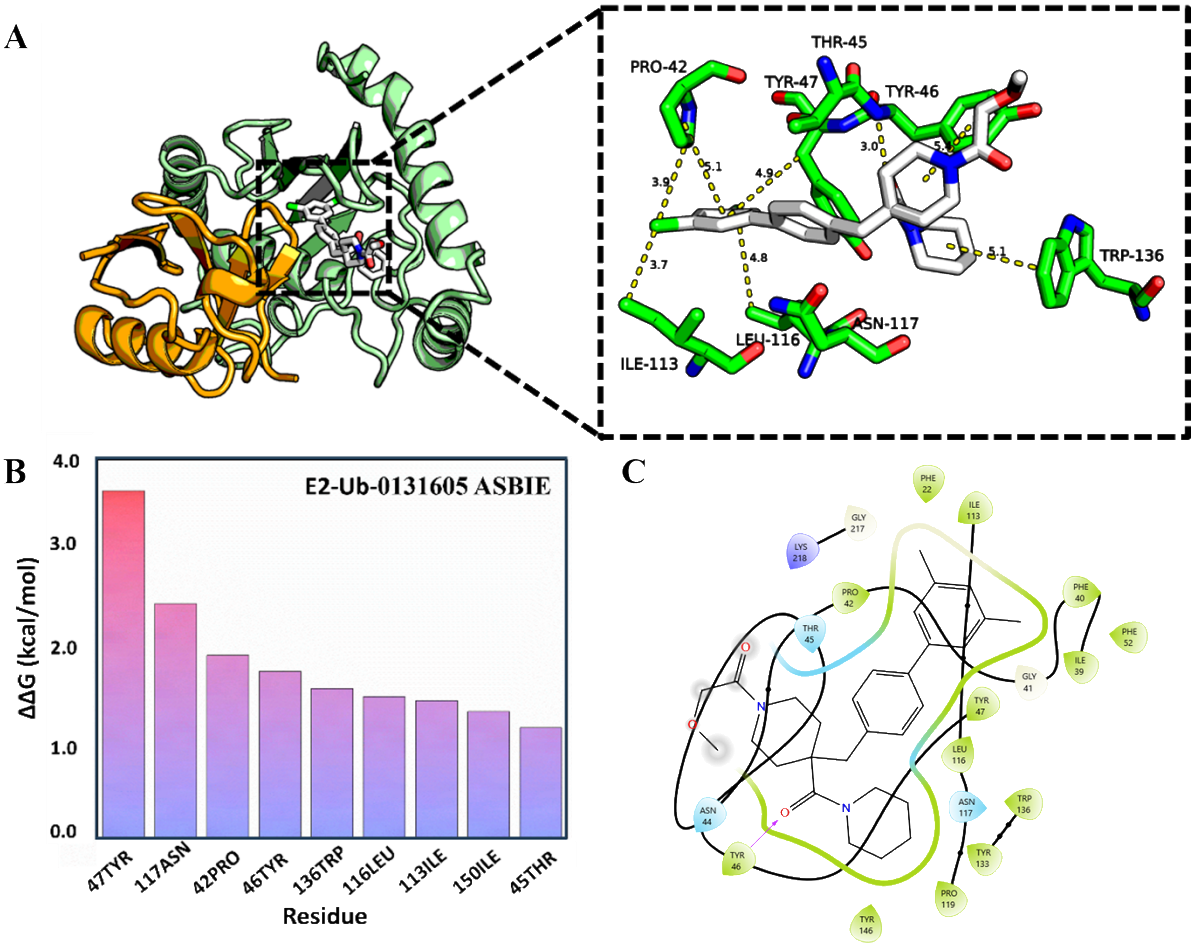

Fig. 3. Residue-Specific Interactions Between E2-Ub and Compound 131605. (A) Bar chart illustrating the average contributions of E2-Ub pocket residues to the binding of compound 0131605. Only residues with a ΔΔG greater than 1.0 kcal/mol are included. **(B)** Interaction diagram highlighting the pocket residues of E2-Ub in contact with compound 131605. Residues predominantly involved in vdW and electrostatic interactions are colored in blue. **(C)** Schematic representation of the 2D interactions between molecular glue (compound 131605) and the hotspot residues of the protein.

3.3. All-atom insights into protein-protein interactions.

A more important feature of the E2-Ub-MG multimeric complex is the MG-induced strengthening of E2-Ub coordination. We therefore present the interfacial contacts in Fig. 4A and probe the ASGB-IE energetics in the E2-Ub pair in the presence and absence of MG in Fig. 4B. The presence of MG incurs significant increases in binding strengths of multiple key residues. For instance, residue 110LEU demonstrates a marked increase in $\Delta\Delta G_{bind}^{x\to a}$ from 1.26 kcal/mol in the

absence of glue, to 2.91 kcal/mol when molecular glue is present. Similarly, residue 20GLU exhibits a shift from a relatively minimal 0.45 kcal/mol to a more substantial 2.40 kcal/mol under the influence of molecular glue. Such MG-induced PPI augmentation is also reflected in the structural packing. In Fig. 4C, we show the intermolecular packing (contact number, to be specific) of the top-3 hot spots in Fig. 4B, where the intermolecular coordinations of these hot residues are strengthened. The structural comparison shown in Fig. 4D suggests a similar trend. These observations provide the structural foundation of the ASGB-IE energetics and validates the reasonableness of our computational workflow.

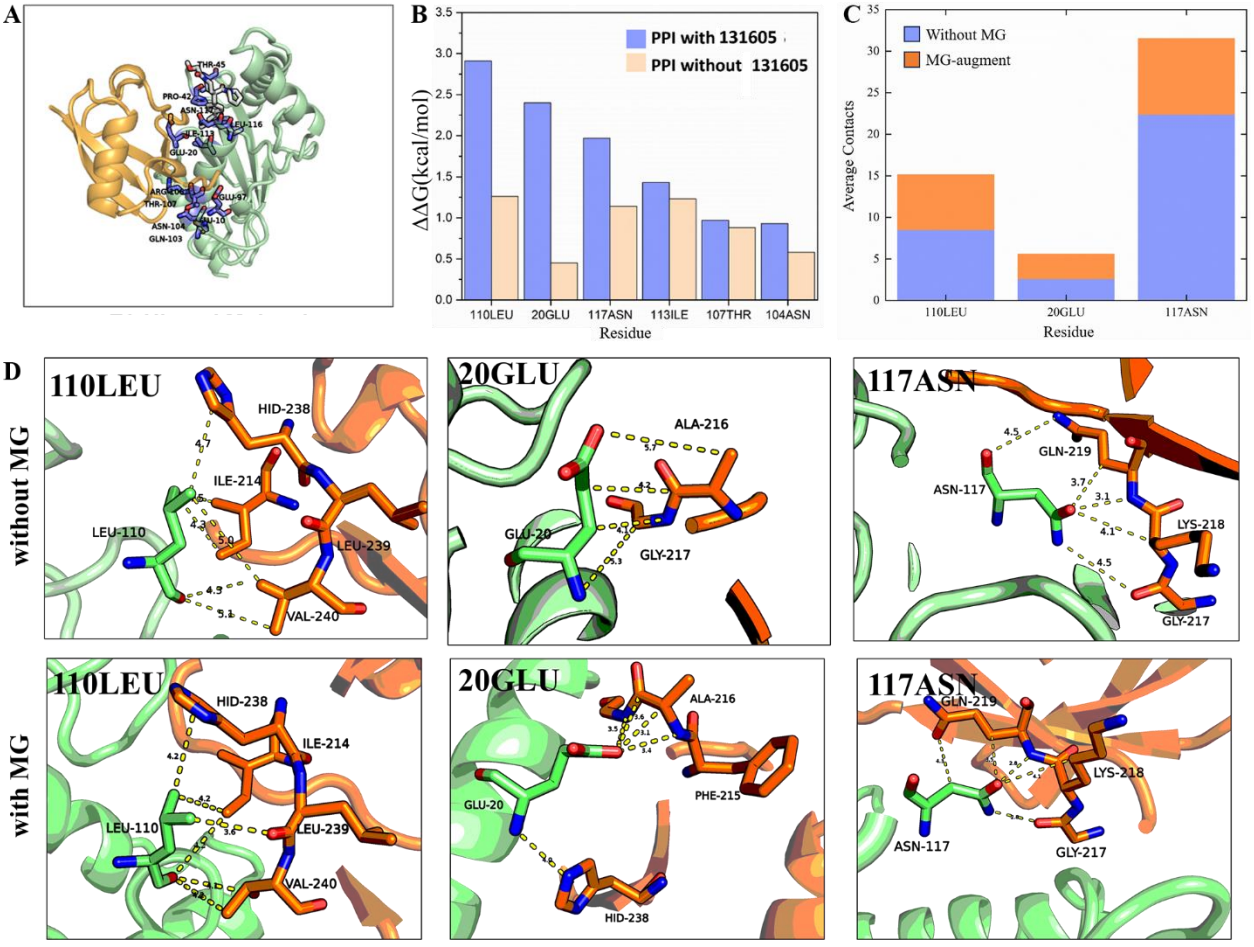

Fig. 4. Comparative Analysis and Structural Representation of E2-Ub Interactions. A) Co-crystal structure of E2-Ub complexed with compound 131605, with E2 highlighted in pale green, Ub in orange, MG in silver and interfacial residues in the stick presentation. B) Energetic contributions to PPI stabilization with and without the 131605 MG. The top-3 hot spots are all on the E2 chain. C) Intermolecular protein-protein packing measured by contact numbers for the

top-3 hot spots in the presence and absence of MG and D) the corresponding structural comparison.

3.4. A general picture of the multimeric E2-Ub-MG interaction.

The above analyses of protein-ligand (protein-glue) and protein-protein interactions provide some basic insights into the coordination features in the multimeric system. In order to extract a general picture of the complex multimeric protein-protein-ligand interaction, in this section we extract the general interaction maps from energetics of all protein-ligand and protein-protein pairs.

As depicted in Fig. 5A, on the protein-ligand interface, 10 residues (47TYR, 117ASN, 42PRO, 46TYR, 116LEU, 136TRP, 45THR, 113ILE, 146TYR, and 150ILE) exhibit significant energetic contributions to the protein-MG binding, with average energies of 57.72, 38.68, 36.32, 29.73, 28.81, 26.13, 23.03, 17.83, 16.34, and 15.68 kcal/mol, respectively (see supplementary tables). Among them, a clear picture of structural features is that smaller and aromatic substituents contribute significantly to binding through π-π stacking and hydrophobic interactions, e.g., the top-4 residues in the above list 47TYR, 116LEU, 42PRO, and 117ASN. Notably, only a single residue of Ub presents on this list, i.e., 218LYS, which is expected as from a structural perspective MG interacts mostly with E2 residues. A decomposition of the chain-specific protein-MG binding affinity is shown in Fig. S2, where the major role of E2 in stabilizing MG is clear. This fact actually makes the impact of MG binding similar to an allosteric effect.

As for the protein-protein packing, we consider both the absence and presence of MG, as shown in Fig. 5B. In the E2-Ub complex (i.e., without MG), 110LEU, 113ILE, 107THR and 104ASN provide the largest portions of stabilization effects. By contrast, with the addition of MG, many other residues especially 117ASN and 20GLU begin to exhibit noticeable stabilizing effects. Such a trend is generally systematic across all MG molecules, although the 131247 MG exhibits slightly different behavior for 20GLU and different residues experience different levels of energetic elevations (or penalties depending of the sign). Therefore, the general picture of the MG-induced increase of E2-Ub affinities could be attributed to the contributions of these key resides lying at the protein-protein interface.

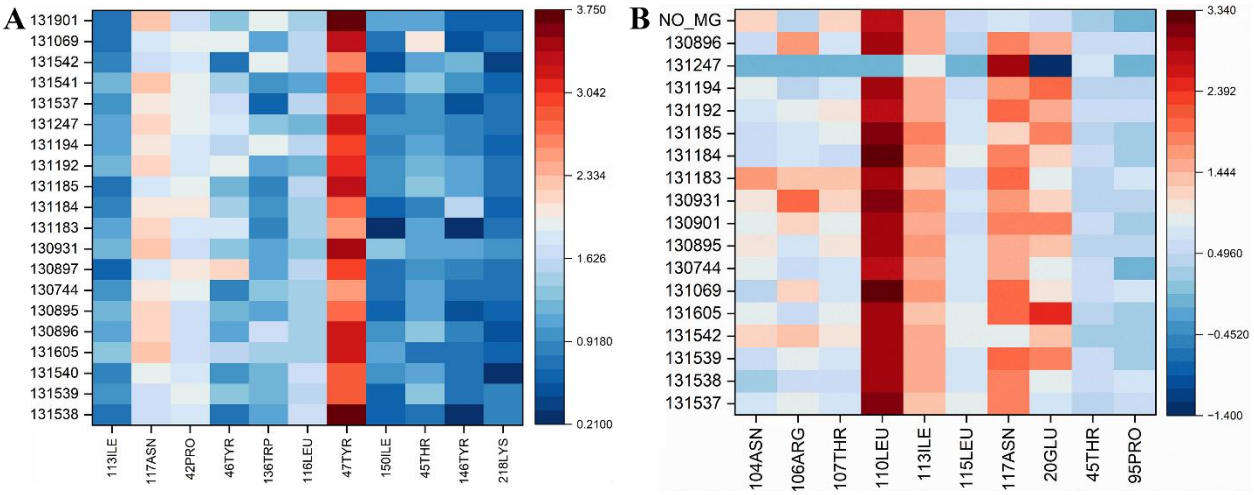

Fig. 5. Heatmaps of residue-specific energetic contributions: A) the MG-(E2-Ub) (protein-ligand) pairs, B) the E2-Ub (protein-protein) pair in the absence and presence of MG. The unit of energy used in coloring is kcal/mol.

4. Concluding Remarks.

Accurate modelling of molecular glues in stabilizing the E2-Ub complex and in general PPI is difficult. The problem lies in the multimeric nature of the protein-protein-ligand complex and its complicated components, which poses difficulties in computational approaches working well in only a single area. In this work, we explore the possibilities of employing a generalized ASGB-IE workflow to handle such multimeric E2-Ub-MG complexes. The numerical results reveal that our method could not only rank protein-ligand affinities with a high accuracy and qualitatively capture MG-induced stabilization effects on a residue-specific level. By contrast, this is unachievable with standard methods like MM/GBSA and scoring functions (AutoDock families and PRODIGY-LIG). This approach provides a comprehensive SAR analysis, pinpointing key residues such as 42PRO, 46TYR, and 47TYR in the E2 protein as major contributors to protein-MG binding, while Ub provides little contribution to the binding of MG. The enhancement of PPI by MG can be quantitatively predicted by computation, but its experimental measurement is not trivial. The presence of molecular glue enhances hydrophobic interactions and aromatic π-π stacking, reinforcing the stability of the ternary complex. We further extended the investigation into exploring the general picture of MG-(E2-Ub) protein-ligand and E2-Ub (protein-protein) complexes. These findings elucidate the mechanisms by which molecular glues promote selective protein degradation, a promising strategy for cancer therapeutics. Although experimental

validation of MG-induced cooperativity is limited, our results underscore the utility of molecular glues in rational drug design, offering new pathways for disrupting oncogenic protein interactions and advancing targeted anti-cancer therapies.

Finally, it should be fair to note the limitation of the current study. In the current work, only one of the 18 MG-E2-Ub complexes has experimental complex structure and the other 17 systems are modelled with homology modeling. This could be a limitation of current workflows for the virtual screening of MG, which could be aided by the fusion of deep learning and physics-based modelling. For example, integrative deep-learning tools for biomolecular complexes (e.g., AlphaFold3) could be applied to provide initial 3D structural models of the multimeric complexes, enabling a fully computational workflow for the discovery and design of promising MG.

Supporting Information

The detailed energetic components of all E2-Ub-MG ASGB-IE scans and a convergence check of all computed PPI strengths are provided in the supporting information.

Acknowledgement

This work was supported by National Natural Science Foundation of China (No. 92270001, 21933010, 22250710136, 22333006).

Data and Software Availability

All generated data including the detailed component-specific ASGB-IE energetics are presented in the supporting information.

Conflict of Interest Statement

There are no conflicts of interest to declare.

References

1. Sung, H.; Ferlay, J.; Siegel, R. L.; Laversanne, M.; Soerjomataram, I.; Jemal, A.; Bray, F., Global Cancer Statistics 2020: GLOBOCAN Estimates of Incidence and Mortality Worldwide for 36 Cancers in 185 Countries. *CA Cancer J Clin* **2021**, 71, 209-249.
2. Siegel, R.; Naishadham, D.; Jemal, A., Cancer statistics, 2013. *CA Cancer J Clin* **2013**, 63, 11-30.
3. Cheng, H.; Planken, S., Precedence and Promise of Covalent Inhibitors of EGFR and KRAS for Patients with Non-Small-Cell Lung Cancer. *ACS Med Chem Lett* **2018**, 9, 861-863.
4. Renaud, S.; Seitlinger, J.; Massard, G., MicroRNAs: a new tool in the complex biology of KRAS mutated non-small cell lung cancer? *J Thorac Dis* **2017**, 9, 957-960.
5. Wang, J. B.; Huang, X.; Li, F. R., Impaired dendritic cell functions in lung cancer: a review of recent advances and future perspectives. *Cancer Commun (Lond)* **2019**, 39, 43.
6. Rape, M., Ubiquitylation at the crossroads of development and disease. *Nat Rev Mol Cell Biol* **2018**, 19, 59-70.
7. Mata-Cantero, L.; Lobato-Gil, S.; Aillet, F.; Lang, V.; Rodriguez, M. S. The Ubiquitin-Proteasome System (UPS) as a Cancer Drug Target: Emerging Mechanisms and Therapeutics. In *Stress Response Pathways in Cancer: From Molecular Targets to Novel Therapeutics*, Wondrak, G. T., Ed.; Springer Netherlands: Dordrecht, 2015, pp 225-264.
8. Yuan, T.; Yan, F.; Ying, M.; Cao, J.; He, Q.; Zhu, H.; Yang, B., Inhibition of Ubiquitin-Specific Proteases as a Novel Anticancer Therapeutic Strategy. *Frontiers in Pharmacology* **2018**, 9.
9. Eldridge, A. G.; O'Brien, T., Therapeutic strategies within the ubiquitin proteasome system. *Cell Death Differ* **2010**, 17, 4-13.
10. Pagano, M.; Tam, S. W.; Theodoras, A. M.; Beer-Romero, P.; Del Sal, G.; Chau, V.; Yew, P. R.; Draetta, G. F.; Rolfe, M., Role of the Ubiquitin-Proteasome Pathway in Regulating Abundance of the Cyclin-Dependent Kinase Inhibitor p27. *Science* **1995**, 269, 682-685.
11. Tanaka, K.; Kondoh, N.; Shuda, M.; Matsubara, O.; Imazeki, N.; Ryo, A.; Wakatsuki, T.; Hada, A.; Goseki, N.; Igari, T., et al., Enhanced expression of mRNAs of antisecretory factor-1, gp96, DAD1 and CDC34 in human hepatocellular carcinomas. *Biochim Biophys Acta* **2001**, 1536, 1-12.
12. Price, G. R.; Armes, J. E.; Ramus, S. J.; Provenzano, E.; Kumar, B.; Cowie, T. F.; Ciciulla, J.; Hutchins, A. M.; Thomas, M.; Venter, D. J., Phenotype-directed analysis of genotype in early-onset, familial breast cancers. *Pathology* **2006**, 38, 520-7.
13. Zhao, X. C.; Wang, G. Z.; Wen, Z. S.; Zhou, Y. C.; Hu, Q.; Zhang, B.; Qu, L. W.; Gao, S. H.; Liu, J.; Ma, L., et al., Systematic identification of CDC34 that functions to stabilize EGFR and promote lung carcinogenesis. *EBioMedicine* **2020**, 53, 102689.
14. St-Cyr, D.; Ceccarelli, D. F.; Orlicky, S.; van der Sloot, A. M.; Tang, X.; Kelso, S.; Moore, S.; James, C.; Posternak, G.; Coulombe-Huntington, J., et al., Identification and optimization of molecular glue compounds that inhibit a noncovalent E2 enzyme–ubiquitin complex. *Science Advances* 7, eabi5797.
15. Burgoyne, N. J.; Jackson, R. M., Predicting protein interaction sites: binding hot-spots in protein-protein and protein-ligand interfaces. *Bioinformatics* **2006**, 22, 1335-42.
16. Chen, J.; Ma, X.; Yuan, Y.; Pei, J.; Lai, L., Protein-protein interface analysis and hot spots identification for chemical ligand design. *Curr Pharm Des* **2014**, 20, 1192-200.

17. Zhong, L.; Li, Y.; Xiong, L.; Wang, W.; Wu, M.; Yuan, T.; Yang, W.; Tian, C.; Miao, Z.; Wang, T., et al., Small molecules in targeted cancer therapy: advances, challenges, and future perspectives. *Signal Transduction and Targeted Therapy* **2021**, 6, 201.
18. Huang, H.; Ceccarelli, D. F.; Orlicky, S.; St-Cyr, D. J.; Ziemba, A.; Garg, P.; Plamondon, S.; Auer, M.; Sidhu, S.; Marinier, A., et al., E2 enzyme inhibition by stabilization of a low-affinity interface with ubiquitin. *Nat Chem Biol* **2014**, 10, 156-163.
19. Schreiber, S. L., The Rise of Molecular Glues. *Cell* **2021**, 184, 3-9.
20. Wang, X., Conformational Fluctuations in GTP-Bound K-Ras: A Metadynamics Perspective with Harmonic Linear Discriminant Analysis. *J. Chem. Inf. Model.* **2021**, 61, 5212-5222.
21. Wang, X.; Chong, B.; Sun, Z.; Ruan, H.; Yang, Y.; Song, P.; Liu, Z., More is simpler: Decomposition of ligand‐binding affinity for proteins being disordered. *Protein Science* **2022**, 31, e4375.
22. Procacci, P.; Chelli, R., Statistical Mechanics of Ligand–Receptor Noncovalent Association, Revisited: Binding Site and Standard State Volumes in Modern Alchemical Theories. *J. Chem. Theory Comput.* **2017**, 13, 1924-1933.
23. Procacci, P., Hybrid MPI/OpenMP Implementation of the ORAC Molecular Dynamics Program for Generalized Ensemble and Fast Switching Alchemical Simulations. *J. Chem. Inf. Model.* **2016**, 56.
24. Procacci, P., Dealing with Induced Fit, Conformational Selection, and Secondary Poses in Molecular Dynamics Simulations for Reliable Free Energy Predictions. *J. Chem. Theory Comput.* **2023**, 19, 8942-8954.
25. Macchiagodena, M.; Pagliai, M.; Procacci, P., NE-RDFE: A protocol and toolkit for computing relative dissociation free energies with GROMACS between dissimilar molecules using bidirectional nonequilibrium dual topology schemes. *J. Comput. Chem.* **2023**, 44, 1221-1230.
26. Procacci, P., Methodological uncertainties in drug-receptor binding free energy predictions based on classical molecular dynamics. *Curr. Opin. Struct. Biol.* **2021**, 67, 127-134.
27. Meng, L.; Xinguo, L.; Shaolong, Z.; Jiahao, S.; Qinggang, Z.; Jianzhong, C., Selective Mechanism of Inhibitors to Two Bromodomains of BRD4 Revealed by Multiple Replica Molecular Dynamics Simulations and Free Energy Analyses. *Chinese Journal of Chemical Physics* **2022**, 1-15.
28. Chen, J.; Zeng, Q.; Wang, W.; Sun, H.; Hu, G., Decoding the Identification Mechanism of an SAM-III Riboswitch on Ligands through Multiple Independent Gaussian-Accelerated Molecular Dynamics Simulations. *J. Chem. Inf. Model.* **2022**.
29. Liu, X.; Peng, L.; Zhang, J. Z., Accurate and Efficient Calculation of Protein–Protein Binding Free Energy-Interaction Entropy with Residue Type-Specific Dielectric Constants. *J. Chem. Inf. Model.* **2018**, 59, 272-281.
30. Yan, Y.; Yang, M.; Ji, C. G.; Zhang, J. Z., Interaction entropy for computational alanine scanning. *J. Chem. Inf. Model.* **2017**, 57, 1112-1122.
31. St-Cyr, D.; Ceccarelli, D. F.; Orlicky, S.; van der Sloot, A. M.; Tang, X.; Kelso, S.; Moore, S.; James, C.; Posternak, G.; Coulombe-Huntington, J., et al., Identification and optimization of molecular glue compounds that inhibit a noncovalent E2 enzyme-ubiquitin complex. *Science Advances* **2021**, 7, eabi5797.
32. Sun, Z.; Yan, Y. N.; Yang, M.; Zhang, J. Z., Interaction Entropy for Protein-Protein Binding. *J. Chem. Phys.* **2017**, 146, 124124.

33. Onufriev, A.; Bashford, D.; Case, D. A., Exploring protein native states and large-scale conformational changes with a modified generalized born model. *Proteins: Struct. Funct. Bioinform.* **2004**, 55, 383-94.
34. Feig, M.; Onufriev, A.; Lee, M. S.; Im, W.; Case, D. A., Performance comparison of generalized born and Poisson methods in the calculation of electrostatic solvation energies for protein structures. *J. Comput. Chem.* **2004**, 25, 265-84.
35. Weiser, J.; Shenkin, P. S.; Still, W. C., Approximate atomic surfaces from linear combinations of pairwise overlaps (LCPO). *J. Comput. Chem.* **1999**, 20, 217-230.
36. Gerber, P. R.; Müller, K., MAB, a generally applicable molecular force field for structure modelling in medicinal chemistry. *Journal of Computer-Aided Molecular Design* **1995**, 9, 251-268.
37. Maier, J. A.; Martinez, C.; Kasavajhala, K.; Wickstrom, L.; Hauser, K. E.; Simmerling, C., ff14SB: Improving the Accuracy of Protein Side Chain and Backbone Parameters from ff99SB. *Journal of Chemical Theory and Computation* **2015**, 11, 3696-3713.
38. Maier, J. A.; Martinez, C.; Kasavajhala, K.; Wickstrom, L.; Hauser, K. E.; Simmerling, C., ff14SB: Improving the Accuracy of Protein Side Chain and Backbone Parameters from ff99SB. *J. Chem. Theory Comput.* **2015**, 11, 3696-3713.
39. Jakalian, A.; Jack, D. B.; Bayly, C. I., Fast, efficient generation of high‐quality atomic charges. AM1‐BCC model: II. Parameterization and validation. *J. Comput. Chem.* **2002**, 23, 1623-1641.
40. Jakalian, A.; Bush, B. L.; Jack, D. B.; Bayly, C. I., Fast, efficient generation of high‐quality atomic charges. AM1‐BCC model: I. Method. *J. Comput. Chem.* **2000**, 21, 132-146.
41. Joung, I. S.; Cheatham III, T. E., Determination of Alkali and Halide Monovalent Ion Parameters for Use in Explicitly Solvated Biomolecular Simulations. *J. Phys. Chem. B* **2008**, 112, 9020-9041.
42. Joung, I. S.; Cheatham, T. E., Molecular Dynamics Simulations of the Dynamic and Energetic Properties of Alkali and Halide Ions Using Water-Model-Specific Ion Parameters. *J. Phys. Chem. B* **2009**, 113, 13279-13290.
43. Papamokos, G. V.; Tziatzos, G.; Papageorgiou, D. G.; Georgatos, S. D.; Politou, A. S.; Kaxiras, E., Structural role of RKS motifs in chromatin interactions: a molecular dynamics study of HP1 bound to a variably modified histone tail. *Biophys J* **2012**, 102, 1926-1933.
44. Ryckaert, J. P.; Ciccotti, G.; Berendsen, H. J. C., Numerical Integration of The Cartesian Equations of Motion of A System with Constraints: Molecular Dynamics of n -alkanes. *J. Comput. Phys.* **1977**, 23, 327-341.
45. Miyamoto, S.; Kollman, P. A., Settle: An Analytical Version of The SHAKE and RATTLE Algorithm for Rigid Water Models. *J. Comput. Chem.* **1992**, 13, 952-962.
46. Quiroga, R.; Villarreal, M. A., Vinardo: A Scoring Function Based on Autodock Vina Improves Scoring, Docking, and Virtual Screening. *PLOS ONE* **2016**, 11, e0155183.
47. Morris, G. M.; Huey, R.; Lindstrom, W.; Sanner, M. F.; Belew, R. K.; Goodsell, D. S.; Olson, A. J., AutoDock4 and AutoDockTools4: Automated docking with selective receptor flexibility. *J. Comput. Chem.* **2009**, 30, 2785-2791.
48. Kurkcuoglu, Z.; Koukos, P. I.; Citro, N.; Trellet, M. E.; Rodrigues, J. P. G. L. M.; Moreira, I. S.; Roel-Touris, J.; Melquiond, A. S. J.; Geng, C.; Schaarschmidt, J., et al., Performance of HADDOCK and a simple contact-based protein–ligand binding affinity predictor in the D3R Grand Challenge 2. *J. Comput.-Aided Mol. Des.* **2018**, 32, 175-185.